J Paleolimnol
https://doi.org/10.1007/s10933-020-00135-z

ORIGINAL PAPER

Quantification of chlorophyll *a*, chlorophyll *b* and pheopigments *a* in lake sediments through deconvolution of bulk UV–VIS absorption spectra

Andrea Sanchini · Martin Grosjean

Received: 11 July 2019 / Accepted: 23 May 2020

Abstract Assessments of aquatic paleoproduction and pigment preservation require accurate identification and quantification of sedimentary chlorophylls. Using chromatographic techniques to analyze long records at high resolution is impractical because they are expensive and labor intensive. We have developed a new rapid and low-cost approach to infer the concentrations of chlorophyll *a*, chlorophyll *b* and related chlorophyll derivatives (pheopigments *a*) from the mathematical decomposition of UV–VIS measured bulk spectrophotometer absorption spectra of standard solutions and sediment extracts. We validated our method against high-performance liquid chromatography (HPLC) measurements on standard solutions and on varved, anoxic sediment from eutrophic Lake Lugano (Ponte Tresa sub-basin, southern Switzerland), where the history of productivity is relatively well known for the twentieth century. Our mathematical approach quantifies the concentration of chlorophyll *b* (R^2_{adj} = 0.99, RMSEP ~ 5.9%), chlorophyll *a* (R^2_{adj} = 0.98, RMSEP ~ 5.0%), and pyropheophorbide *a* (R^2_{adj} = 0.99, RMSEP ~ 7.8%) in standard solutions. We obtain comparable results for total chloropigment *a* (chlorophyll *a* + pheopigments *a*), chlorophyll *a* and diagenetic products (pheopigments *a*) in the sediment samples of our case study (Ponte Tresa). Here, HPLC concentrations of chlorophyll *b* are very low. The method has, however, the potential to achieve values for chlorophyll *b* concentrations in sediments with chlorophylls *a*/chlorophylls *b* ratios lower than 3.4. The pigment stratigraphy of the Ponte Tresa sediments correspond very well with the paleoproduction and eutrophication history of the twentieth century. The ratio between chlorophyll *a* and pheopigments *a* used as a qualitative indicator of sedimentary chlorophyll preservation (chlorophyll *a*/{chlorophyll *a* + pheopigments *a*}) is only weakly correlated with aquatic paleoproduction (r_{adj} = 0.35, *p*-value = 0.045) and remained remarkably constant in the recent century despite strong anthropogenic eutrophication. The new method is useful for obtaining, in a cost- and time-efficient way, information about major sedimentary pigment groups that are relevant to inferring paleoproduction, potentially green algae biomass, pigment preservation and early diagenetic effects.

Electronic supplementary material The online version of this article (https://doi.org/10.1007/s10933-020-00135-z) contains supplementary material, which is available to authorized users.

A. Sanchini (✉)
Institute of Geography, University of Bern, Hallerstrasse 12, 3012 Bern, Switzerland
e-mail: andrea.sanchini@giub.unibe.ch

M. Grosjean
Oeschger Centre for Climate Change Research, University of Bern, 3012 Bern, Switzerland
e-mail: martin.grosjean@oeschger.unibe.ch

Published online: 09 June 2020

Keywords Sedimentary pigments · UV–VIS absorption spectra · Deconvolution · Aquatic paleoproduction · Chlorophyll preservation index

Introduction

Sedimentary algal and bacterial pigments have been used for decades to gather information about algal communities, aquatic productivity, eutrophication, redox (e.g. meromixis), food web and light conditions, and water temperatures in lakes (Züllig 1982; Lami et al. 2009; Bianchi and Canuel 2011). Sedimentary chlorophyll *a* (chl *a*) and chlorophyll derivatives (pheopigments *a*, pheo *a*) are widely used as a proxy for past phytoplankton biomass production (Bianchi and Canuel 2011; McGowan 2013). Information about paleoproduction is important to understand the magnitude and variability of natural and anthropogenic eutrophication, nutrient cycling and temperature changes in aquatic systems through time (Belle et al. 2018).

Chloropigments (chls, the sum of chl and pheo) are labile molecules and a variety of transformation products, such as pheophytin *a*, pyropheophytin *a*, pyropheophorbide *a*, pheophorbide *a,* are readily formed during chemical and biological processes in lakes including cellular senescence, photo oxidation and microbial oxidation, herbivore grazing, among others (Leavitt 1993; Bianchi and Canuel 2011). Most chloropigments in the euphotic zone are degraded through photo oxidation and enzymatic degradation to colorless compounds (Rutherford 1989; Brown et al. 1991; Nugent 1996; Buchaca and Catalan 2008). Some specific pheopigments *a* have been used as indicators of zooplankton grazing. For instance, pheophorbide *a* (phide *a*) was found in protozoan fecal pellets (Bianchi and Canuel 2011) and pyropheophorbide *a* (pyrophide *a*) was found in copepod fecal pellets (Bianchi and Canuel 2011).

Several authors used the ratios between chlorophylls and chlorophyll derivatives to assess the degree of pigment degradation and organic matter freshness. Buchaca and Catalan (2008), for instance, introduced the Chlorophyll Preservation Index (CPI) (chl *a*/{chl *a* + pheopigments *a*}), Deshpande et al. (2014) used the ratio chl *a*/pheophytin *a*, and Schubert et al. (2005) established the Chlorin Index to assess organic matter freshness in sediments.

Nowadays, the identification and quantification of sedimentary pigments is mostly obtained through advanced analytical techniques such as high-performance liquid chromatography (HPLC) and gas chromatography (GC). These techniques are highly compound specific but they require high levels of expertise, labor and costs. In consequence, long-term (e.g. Holocene) reconstructions are limited by the temporal resolution and number of samples that can be processed in a reasonable time. Multi-lake studies are very rare (Schubert et al. 2005).

To overcome these limitations, several researchers have explored and developed more inexpensive and rapid methods either to measure bulk chloropigments directly from lake sediments using VIS-VNIR reflectance spectroscopy (Butz et al. 2015; Michelutti and Smol 2016) or to quantify specific chloropigments in synthetic and natural matrices using spectrophotometric measurements of sediment extracts (Wetzel 1970; Jeffrey and Humphrey 1975; Lichtenthaler and Buschmann 2001; Ritchie 2008). These latter approaches apply mostly empirical or theoretical linear equations (mono-di-trichroic equations) to the bulk spectrophotometric absorption spectra to infer specific chloropigment concentrations in extracts. However, these approaches tend to overestimate the concentrations of the parent chloropigments (chl *a*, chl *b*) in the presence of diagenetic compounds (Ritchie 2008). Acidification techniques were proposed to correct for the inaccuracy of universal algorithms (Lichtenthaler 1987; Jeffrey et al. 1997). Despite this further correction, the estimated concentration still may be incorrect because (1) chl needs to be completely converted to 100% pheopigments through acidification (Jeffrey et al. 1997) and, (2) the background absorption needs to remain constant before and after the acidification, which is mostly not the case as acidification leads to turbidity (Küpper et al. 2007).

Recently, a different method has been developed with the aim to deconstruct the bulk absorption spectrum of extracted samples as a weighted sum of individual components through spectral deconvolution (Naqvi et al. 2004; Küpper et al. 2007; Thrane et al. 2015). This approach was applied for the first time on lake sediment cores by Thrane et al. (2015), who were able to correctly infer total chloropigment concentrations. However, as mentioned above, a more

species-specific identification and accurate quantification of chloropigments and their related pheopigments is needed to better understand aquatic paleoproduction, green algae biomass and chloropigments preservation.

In this study, we developed a new method to quantify important chloropigment species in lake sediments from bulk UV–VIS spectrophotometer absorption spectra using spectral deconvolution. Our specific study goals were to develop a fast and inexpensive alternative to existing methods for the simultaneous quantification of (1) chl *a* [an indicator of aquatic paleoproduction (Bianchi and Canuel 2011)], (2) chl *b* [an indicator of green algae biomass (Jeffrey et al. 1997)], and (3) pheo *a*, which combined with chl *a* allows the calculation of the Chlorophyll Preservation Index (Buchaca and Catalan 2008) that is used to assess (early) diagenetic effects in surface sediments and pigment preservation through time. We test and validate our method on standard solutions and on lake sediment samples collected from a sediment core in the Ponte Tresa sub-basin of Lake Lugano, Switzerland. This lake was chosen because its eutrophication history is well documented (Schneider et al. 2018) and pigments are thought to be well preserved in anoxic sediments (Reuss and Conley 2005).

Study site

Lake Lugano, southern Switzerland (Fig. 1) is of fluvio-glacial tectonic origin. The Ponte Tresa sub-basin has a surface area of 1.1 km^2, a volume of 0.03 km^3, a maximum depth of 51 m, and is currently eutrophic (Simona 2003). The Ponte Tresa basin receives most of its water from Lake Lugano. The mean water residence time is 0.04 years and the Tresa River is its only outflow (annual discharge of 0.75 km^3; Simona 2003). The regional climate is temperate (Köppen classification) and characterized by mild winters, and warm and humid summers (Niessen 1987). The catchment area is highly industrialized and populated in the lowlands and along the lake shores, whereas the rest of the watershed is mostly covered by mixed deciduous forest.

Sediments deposited during the twentieth century are varved (biochemical varves) and anoxic (Züllig 1982). The sediment composition, core chronology and eutrophication history is well documented in Schneider et al. (2018). A first increase in aquatic productivity was observed after 1930 followed by its maximum around 1964 and 1990 when the lake was highly eutrophic. Afterwards, wastewater treatment was widely implemented and the eutrophication process started to slowly decline but remained at very high levels. Despite the restoration measurement aimed at improving environmental water quality,

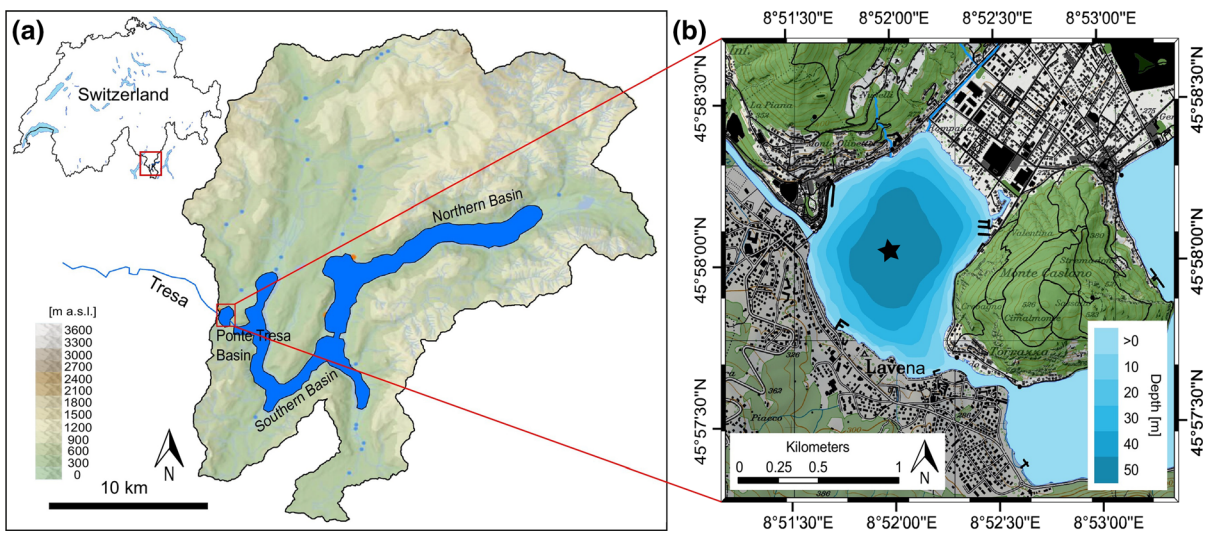

Fig. 1 **a** Location of Lake Lugano within Switzerland and the Ponte Tresa sub-basin (red rectangle). **b** Bathymetric map of Ponte Tresa sub-basin. The black asterisk marks the coring site (figure from Schneider et al. 2018). (Color figure online)

episodes of very high production with algal blooms were still observed in the last decade due to internal nutrient cycling of the lake (Schneider et al. 2018; Tu et al. 2019).

Materials and methods

Sediment sampling

We collected a short sediment core (PTRE 17-5-A) with an UWITEC gravity corer from the deepest zone of the Ponte Tresa basin (45°58′ 02″ N; 8°52′ 00″ E, coring site in Fig. 1b) in September 2017. After collection, the core was stored at 4 °C in a dark room. The core was then split lengthwise and stratigraphically correlated with the dated core (PTRE-15-3-A, Electronic Supplementary Material, ESM1) described in Schneider et al. (2018). For the pigment analysis, 25 subsamples were taken at 2-cm contiguous intervals (sample resolution about 4 years) back to an age of 1914.

Standard solution preparation

In this article we use the pigment terminology according to Bianchi and Canuel (2011) and pigment abbreviations according to Welschmeyer (1994) and Jeffrey et al. (1997).

We prepared seven standard solutions with different concentrations of chl *a* and chl *b*. Two solutions consisted of pure substances (chl *a* and chl *b*, respectively) whereas the other five solutions contained concentration ratios (chl *a*/chl *b*) that range from 3.41 to 0.16 (Routh et al. 2009; Ramanathan et al. 2012; Waters et al. 2013; Mikomägi et al. 2016; Makri et al. 2019). In the standard solutions, the concentration of chl *a* and chl *b* spanned from 1.20 to 6.10 mg L^{-1} and from 1.79 to 7.53 mg L^{-1}, respectively.

We also prepared four standard solutions with chl *a* and pyropheophorbide *a* (i.e., a derivative of chl *a*). The concentrations of chl *a* spanned from 1.81 to 5.37 mg L^{-1}, whereas that of pyropheophorbide *a* spanned from 2.41 to 8.78 mg L^{-1}. Concentration ratios varied from 2.34 to 0.21 (chl *a*/pyropheophorbide *a*). Typical values for chl *a*/pheopigments *a* found in eutrophic and oligotrophic lakes range between 2.5 and 0.5 (Guilizzoni et al. 1992; Dreßler et al. 2007; Makri et al. 2019).

Extraction and measurement methods for sedimentary pigments

The samples were extracted with a method modified from Reuss and Conley (2005) with acetone 95%. For further details we refer to ESM2.

Chloropigments were analyzed with a UV–VIS spectrophotometer (Shimadzu, UV-1800 CE, 230 V, 300-900 nm) at 0.1-nm step size and with a spectral bandwidth of 1 nm. A Plastic UV-Cuvette micro with 1 cm of optical path (Brand GmbH & Co. KG, Wertheim, Germany) was used. We optimized the z height center by having a total of 400 µL of solvent in the cuvette. The absorbance interval used for chloropigments quantification spanned from 0.25 to 0.9 units. We selected this range because the instrumental response is linearly correlated to concentration, more sensitive and less prone to errors when constrained to this range (Lichtenthaler and Buschmann 2001).

Chloropigment species were analyzed by reversed-phase HPLC modified after Lami et al. (2009), using an Agilent Infinity 1260 series equipped with a G7117C Diode-Array Detection (DAD) detector and a G7121A fluorescence detector (FLD). A solution composed of 25 µL extracted sample in Acetone 100% HPLC grade was injected into an Agilent Technologies column Omnisphere (250 mm × 4.6 mm, 5 µm, Agilent Technologies, Switzerland) through an Omnisphere replacement guard column (10 mm × 3 mm, ChromGuard, Switzerland). The separation was carried out at 25 °C with a solvent gradient as displayed in ESM3. Chloropigments species were identified and quantified with standard compounds (ESM4), setting the DAD detector at different wavelength of absorption (i.e., 432 nm for chl *a*, 468 nm for chl *b* and 408 nm for pheopigments *a* to increase sensitivity). Furthermore, the FLD detector was set at λ_{ex} = 408 nm and λ_{emi} = 668 nm, and at λ_{ex} = 432 nm and λ_{emi} = 668 nm to double check the correct identification of pheopigments *a* and chl *a*.

Peak deconvolution of UV–VIS bulk absorption spectra

In order to make the spectrophotometer measurements more compound specific and accurate, we developed a new approach consisting of two consecutive steps:

Step 1 The spectrophotometric bulk absorption spectrum of sediment extracts (e.g. red line in Fig. 2) is deconvoluted with an iterative non-linear least square (INLLS) fitting (Küpper et al. 2007; O'Haver 2016) into a number of individual peaks (e.g. five peaks in Fig. 2, for illustrative purposes). Those two peaks (orange and green in Fig. 2) that match with their absorption maxima chls *a* and chls *b* are "targeted peaks" whereas the other three peaks (gray lines in Fig. 2) are related to unknown substances or physical artifacts ("untargeted peaks"). Step 1 serves to quantify the two components chls *a* and chls *b* from the bulk spectrum.

Step 2 Dichroic equations are applied to one of the targeted peaks after Step 1 (e.g. chloropigments *a* in Fig. 2) to separate chlorophyll (e.g. chl *a*) from the chlorophyll derivatives (e.g. pheopigments *a*). This step serves to calculate the chlorophyll preservation index.

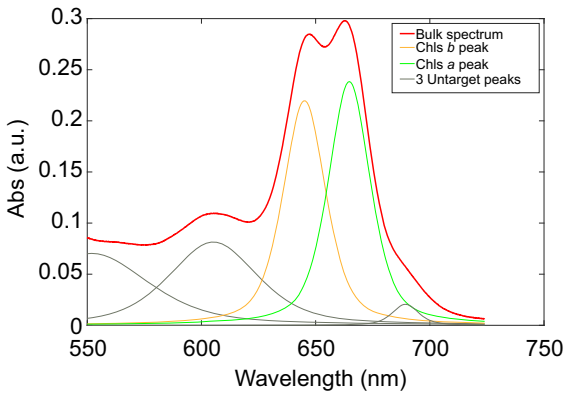

Fig. 2 The bulk UV–VIS spectrum (red line) of a sediment extract of unknown composition is deconvoluted into five peaks using an iterative non-linear least square fitting: the orange and green peaks are characteristic for chloropigments *b* (chls *b*, green algae) and chloropigments *a* (chls *a*, mainly aquatic paleoproduction) whereas the other three peaks (grey lines) represent unknown (non-chlorophyll *a* or *b*) substances or physical artifacts. This sample is for illustrative purposes (i.e. a sediment sample from Ponte Tresa spiked with chl *b*). (Color figure online)

In the following, further details about the two steps of our methodology are provided.

Step 1 The bulk absorption spectrum, $X(\lambda)$ (abs), of a solution as a function of the wavelength λ can be represented by a linear combination of J absorption spectra, $F_j(\lambda)$ (abs):

$$X(\lambda) = \sum_{j=1}^{J} a_j F_j(\lambda) \quad (1)$$

where a_j are the weights defining the contribution of each jth component to the total absorbance. Each jth absorption spectrum can be described with symmetrical or asymmetrical functions, $F_j(\lambda, \delta_j, \omega_j)$, with the peak located at wavelength δ (nm) and the half-width equal to ω (nm).

In order to obtain each jth component of the bulk absorption spectrum, we used the INLLS method (Küpper et al. 2007; O'Haver 2016). The INLLS method fits iteratively the original spectrum, $X(\lambda)$, until the unknown model parameters (i.e., a_j, $\delta_j$and ω_j) are adjusted to minimize the sum-of-squared differences between the observed spectrophotometer, $X_{obs}(\lambda)$, and the calculated absorbance, $X_{cal}(\lambda)$, from the INLLS method (O'Haver 2016):

$$\varepsilon(\lambda) = X_{obs}(\lambda) - X_{cal}(\lambda) \quad (2)$$

We tested seven symmetrical and six asymmetrical functions for describing $F_j(\lambda)$ (ESM5), and found that the Gaussian/Lorentzian blend function performed best compared with the target pigments (highest R^2, smallest root-mean-square deviation RMSD, ESM6). The INLLS method was performed with a freely available peakFit algorithm from the SPECTRUM package (O'Haver 2018) run in MatLab. As input model parameters, we restricted the spectral interval of deconvolution to the range between 550 and 725 nm to avoid interference with carotenoids. Furthermore, we defined the number of peaks per bulk spectrum (4 for standard solutions and 5 for sediment samples), the number of iterations (100) and the instrumental noise (sample standard deviation measured on 10 blank solutions). Tests have shown that a higher number of peaks per bulk spectrum did not improve the results in our samples. The position, width and height of the spectral peaks were not defined, and a baseline correction was not imposed. The concentration c (mg L^{-1}) of chl *b* and chl *a* in standard solutions

and chloropigments *a* in sediment samples are quantified with the Beer–Lambert's law:

$$c = A_\lambda/(\alpha_\lambda \cdot b) \quad (3)$$

where A_λ (abs) is the maximum absorbance at a given λ; α_λ (L cm^{-1} mg^{-1}) is the absorbance coefficient and b is the optical path which, in our case, is 1 cm. In standard solutions, the absorbance coefficient is equal to $\alpha_{645.0} = 51.7 \times 10^{-3}$ L cm^{-1} mg^{-1} for chl *b* (Lichtenthaler 1987) and $\alpha_{662.7} = 88.15 \times 10^{-3}$ L cm^{-1} mg^{-1} for chl *a* (Jeffrey et al. 1997). In sediment samples, chloropigments *a* are quantified using an absorbance coefficient of $a_{666} = 80.77 \times 10^{-3}$ L cm^{-1} mg^{-1} (Jeffrey and Humphrey 1975).

Step 2 The concentrations of chl *a* and pyropheophorphide *a* in standard solutions and chl *a*, and pheopigments *a* in sediment samples are quantified with the following dichroic equations:

$$C_{Chl\,a} = 57.81 \cdot A_{662.7} - 51.92 \cdot A_{666.0} \quad (4)$$

$$C_{Pheo\,a/Pyrophide\,a} = 63.08 \cdot A_{666.0} - 56.44 \cdot A_{662.7} \quad (5)$$

Both dichroic equations were developed after Lichtenthaler and Buschmann (2001) in which we assume that pyropheophorbide *a*, pheophorbide *a*, pheophytin *a* and pyropheophytinp *a* have the same molar extinction coefficient of absorbance at 666.0 nm. In our approach, these four diagenetic pigments in sediment samples are indistinguishable and they are considered as the total pheopigments *a*.

We validate our method by (1) comparing the observed spectrophotometer $X_{obs}(\lambda)$ with the absorbance $X_{cal}(\lambda)$ as calculated from the INLLS method and, (2) by comparing the concentrations of the spectral deconvoluted peaks (SDPs) obtained from Eqs. 3, 4 and 5 with the corresponding concentrations measured with the HPLC. We validate Step 1 with the coefficients of determination (R^2) and root-mean-square deviation (RMSD) and Step 2 with the Adjusted Coefficient of Determination (R^2_{adj}) and root-mean-square error of prediction (RMSEP). In Step 1 and 2 we used R^2 and R^2_{adj} to estimate the match between the experimental values and the values predicted by the deconvolution procedure. To observe the correlation between two predicted variables the adjusted correlation coefficient (r_{adj}) is used.

Results

Method validation with standard solutions

The observed $X_{obs}(\lambda)$ and fitted $X_{cal}(\lambda)$ bulk absorption spectra (Fig. 3a, blue and red lines) are very similar showing RMSD values spanning from 0.4 to 0.8% (mean 0.6%). Residual analyses between the observed and fitted bulk absorption spectra show that the residuals are randomly distributed along the spectral range considered (550–725 nm) (Fig. 3b).

We observe that the deconvoluted peaks (targeted peaks) have their mean maxima at $\lambda_{max} = 662.38$ nm and $\lambda_{max} = 645.90$ nm, which are typical values for chl *a* and chl *b*, respectively (ESM7). Moreover, higher concentrations of chl *a* than chl *b* lead to red-shift in the maximum absorption peak of the bulk spectrum (Fig. 3c). The opposite effect is observed if chl *b* is more abundant than chl *a* (Fig. 3a). Residuals are randomly distributed (Fig. 3b, d).

Figure 4 shows the validation results of the deconvoluted spectral peaks for composite standard solutions obtained from Eqs. 3, 4, 5 and the corresponding pigment concentrations measured with the HPLC. In the standard solutions composed of chl *a* and chl *b*, R^2_{adj} spans between 0.98 and 0.99 (*p*-value $\sim 10^{-5}$, n = 6) with a RMSEP between 5% and 6% (Fig. 4a, b). In standard mixtures of chl *a* and pyropheophorbide *a*, R^2_{adj} is 0.98 (*p*-value $\sim 10^{-3}$, n = 4) and RMSEP between 7 and 11% (Fig. 4c, d). Residual analyses of the standard solutions show that the values are linearly independent (scale-location plot), normally distributed (standardized residuals versus theoretical quantiles and normal Q–Q plots), and no outliers are present based on the Cook's distance (data not shown). The validation of the SDP results with the 'known' pigment concentrations of the standard solutions yielded very similar results (ESM8).

Method validation on sediment samples

In contrast to standard solutions, extracts from environmental matrices (lake sediments) contain many untargeted compounds that may interfere with the identification and quantification of the target species. Therefore, we performed a validation with 25 samples from a lake sediment core of the Ponte Tresa subbasin, southern Swiss Alps. The observed UV–VIS

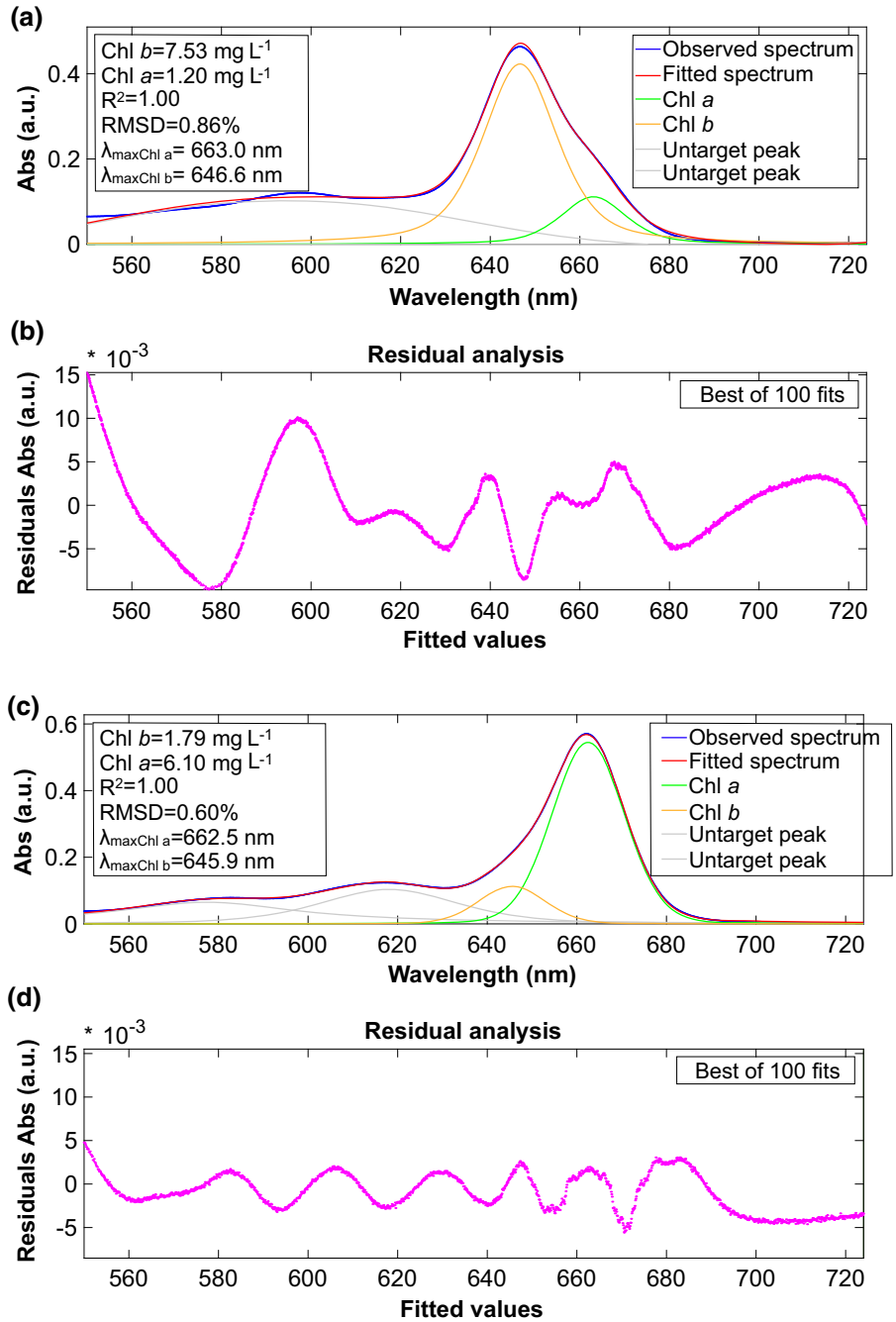

Fig. 3 **a**, **c** Observed UV–VIS bulk spectrum, $X_{obs}(\lambda)$ (blue), fitted spectra, $X_{cal}(\lambda)$ (red), deconvoluted spectra for chl *a* (green), chl *b* (orange), and for two unknown (non-chlorophyll *a* or *b*) substances or physical artifacts (grey); **b**, **d** residuals (pink dots), $X_{obs}(\lambda)$-$X_{cal}(\lambda)$. The results are reported for a standard solution in which chl *b* ≫ chl *a* (**a**) and chl *a* ≫ chl *b* (**c**). (Color figure online)

absorbance spectra (ESM9) and the fitted bulk absorption spectra show a $R^2 > 0.9$ and RMSD between 0.2 and 0.6% with a mean value of 0.3%.

The validation of the results from the spectral deconvolution (SDP obtained from Eqs. 3, 4, 5) with the corresponding pigment concentrations as

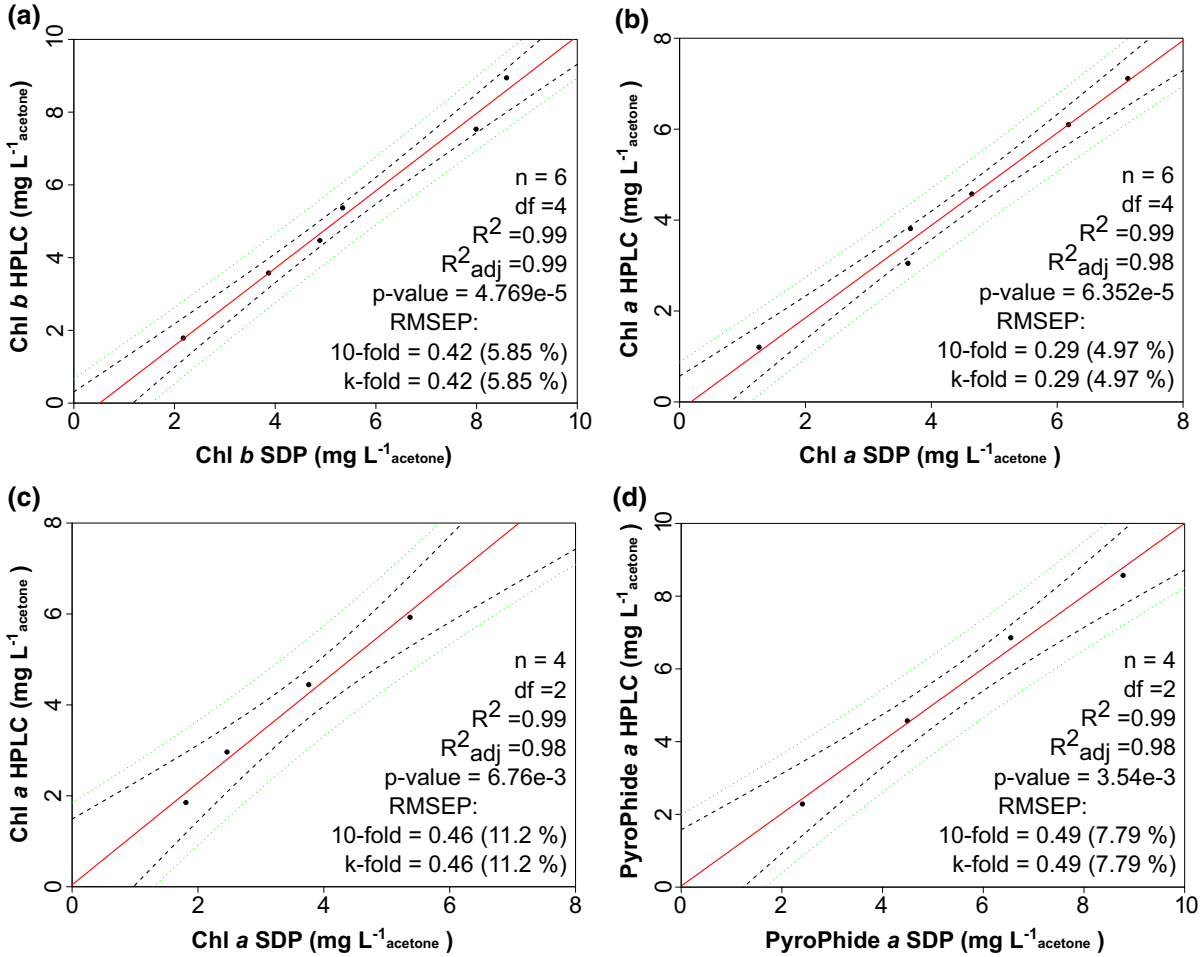

Fig. 4 Method validation between HPLC measured and SDP calculated concentrations for (**a**, **b**) seven standard solutions with mixtures of chl *a* and chl *b* and (**c**, **d**) four standard solutions with mixtures of chl *a* and pyropheorbide *a*. The black dashed lines delimit the 95% confidence interval for the regression function (red) and the green lines indicate the range of the predicted values (green). (Color figure online)

measured with the HPLC (chlorophyll *a*, pyropheophorbide *a*, pheophorbide *a*, pheophytin *a* and pyrophephytin *a*) revealed R^2_{adj} values for chloropigments *a*, chl *a* and pheopigments *a* ranging from 0.98 to 0.99 (p-values $\leq 10^{-20}$) and RMSEP between 3 and 6% (Fig. 5a–c). The diagnostics of the linear regression models for chloropigments *a*, chl *a* and pheopigments *a* show that the values are linearly independent (scale-location plot and residual analysis), normally distributed (standardized residuals versus theoretical quantiles and normal Q–Q plots) and no outliers are present based on the Cook's distance (ESM10, ESM11 and ESM12). In the case of the Ponte Teresa sediment, the INLLS approach was not successful for the quantification of chls *b* because the chls *a*/chls *b* ratio was very high (> 10) and chls *b* concentrations very low (< 10 μg g^{-1}).

Case study from the Ponte Tresa sub-basin (1914–2017)

In our case study, we focus on chlorophyll *a* and diagenetic products. The calculated SDP concentrations of chloropigments *a*, pheopigments *a* and chl *a* agree with the HPLC analyses along the entire sediment profile (Fig. 6a–c). We observe that the concentration of these compounds increases over time (Fig. 6a): the oldest sediment (50 to 34 cm, ca. 1913–1952) is characterized by low chloropigment

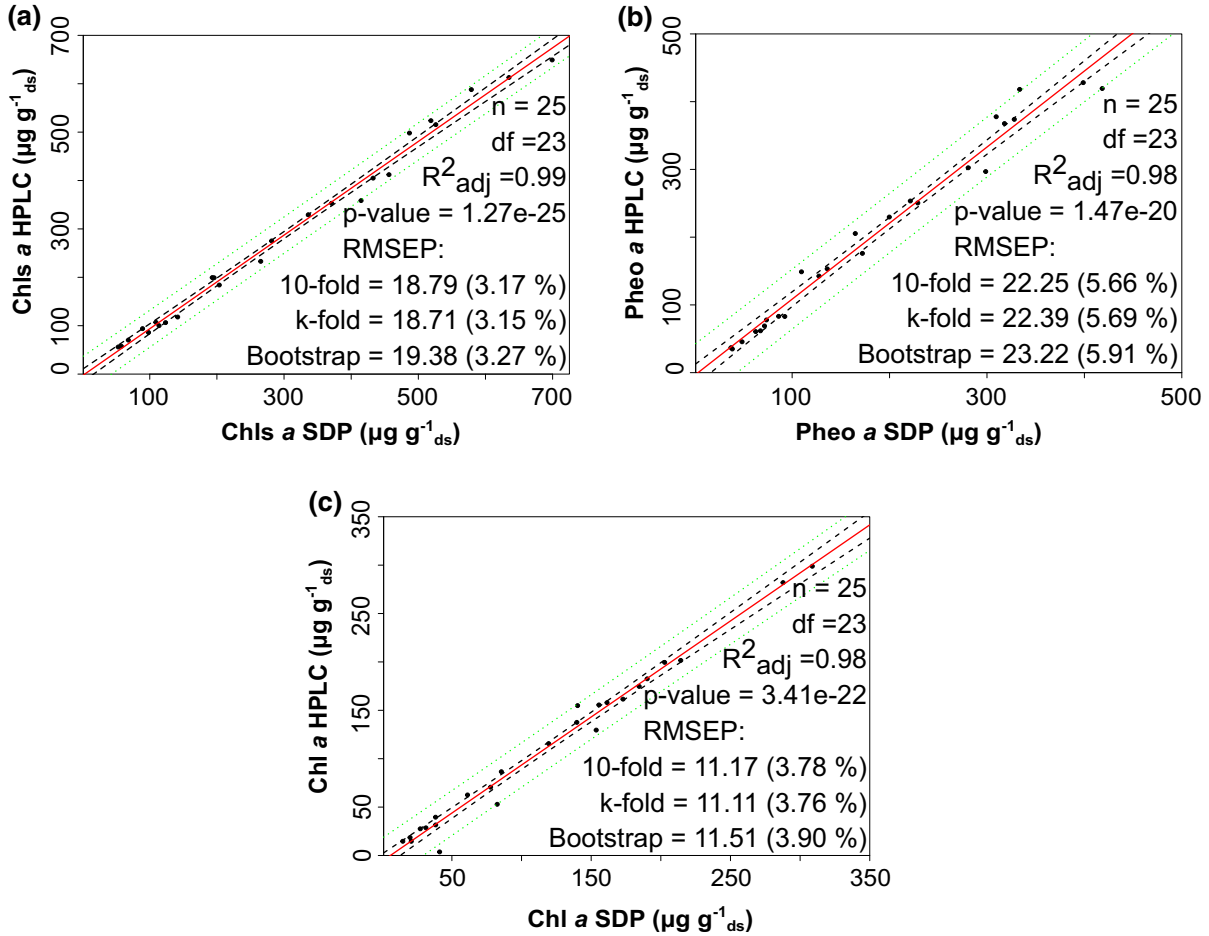

Fig. 5 Method validation between HPLC measured and SDP calculated concentrations for **a** chloropigments *a*, **b** pheopigments *a* and **c** chl *a* in sediment samples of the Ponte Tresa subbasin of Lake Lugano. The black dashed lines delimit the 95% confidence intervals for the regression function (red) and the green lines indicate the range of the predicted values (green). (Color figure online)

a concentrations (mean $c_{chls\ a,SDP}$ = 92 µg g_{ds}^{-1}) and variability, which we attribute to relatively low primary production. At a sediment depth between 34 and 24 cm (ca. 1952–1964), chloropigment *a* concentration doubles (mean $c_{chls\ a,SDP}$ = 175 µg g_{ds}^{-1}) with a local maximum at 34–32 cm (ca. 1952–1955; $c_{chls\ a,SDP}$ = 265 µg g_{ds}^{-1}). The upper part of the sediment core from 24 to 0 cm (ca. 1964–2017) shows the highest chloropigments *a* concentrations (mean $c_{chls\ a,SDP}$ = 460 µg g_{ds}^{-1}) and variability, associated with the highest paleoproduction. We observe three relative chloropigments *a* maxima at 24–20 cm (ca. 1964–1973; $c_{chls\ a,SDP}$ = 503 µg g_{ds}^{-1}), at 14–10 cm (ca. 1987–1993; $c_{chls\ a,SDP}$ = 607 µg g_{ds}^{-1}) and at 2–0 cm (ca. 2010–2017; $c_{chls\ a,SDP}$ = 699 µg g_{ds}^{-1}) (Fig. 6a).

HPLC data reveal that the degradation products of chl *a* are mostly composed of pheophytin *a* ≫ pheophorbide *a* > pyropheophorbide *a* = pyropheophytin *a* (Fig. 6e). The concentrations of pheophytin *a* show a marked increase in the 1950s and around 1968, 1988 and present day; pheophorbide *a* reveals a marked increase around 1988 (± 4 years) and in the last decade, whereas pyropheophorbide *a* and pyropheophytin *a* remain at low levels and remarkably constant over time (Fig. 6e). Pheophytin *a* and chlorophyll *a* are highly correlated with synchronous relative maxima. The proportion of pheophorbide *a* relative to the other pheopigments

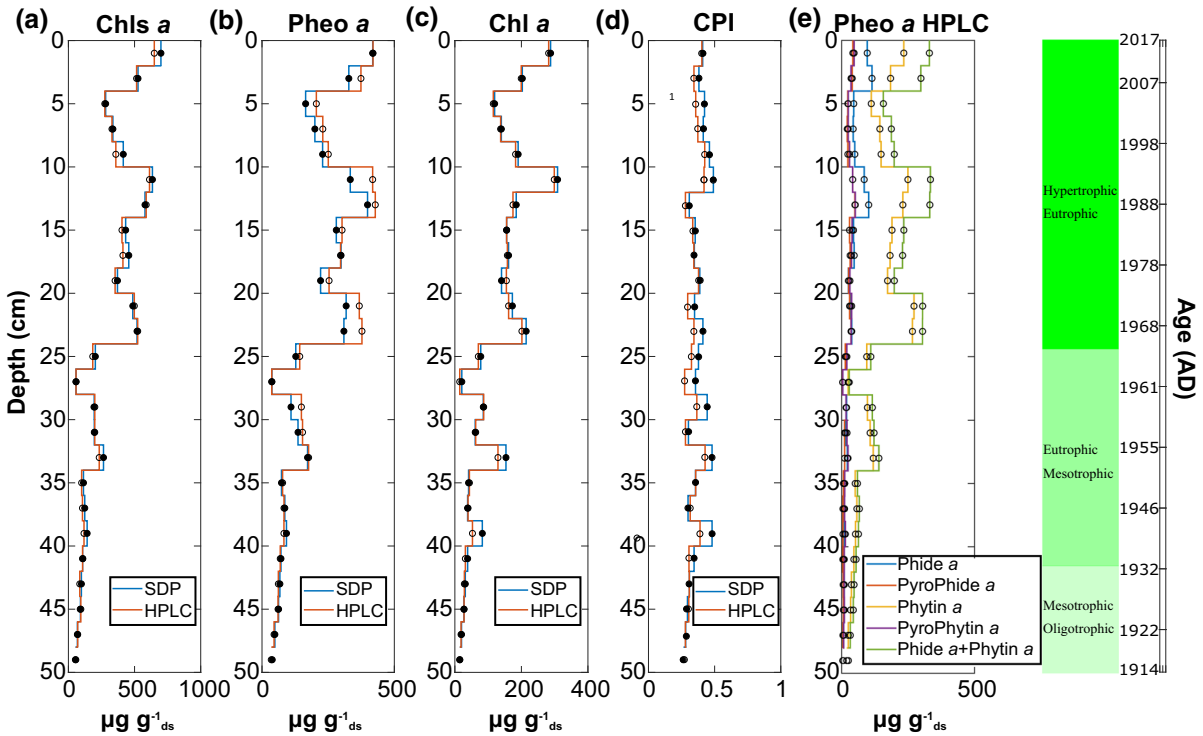

Fig. 6 Pigment stratigraphy of the sediment core PTRE 17-5 (Ponte Tresa sub-basin) showing the comparison between HPLC-measured and SDP-calculated concentrations for **a** chloropigments *a* (chls *a*); **b** pheopigments (pheo *a*); **c** chl *a*, **d** CPI and, **e** specific pheopigments *a*: pyropheophorbide *a* (pyrophide *a*), pheophorbide *a* (phide *a*), pheophytin *a* (phytin *a*) and pyrophephytin *a* (pyrophytin *a*) obtained through HPLC. The green colors show the Ponte Tresa trophic state according to Schneider et al. (2018). (Color figure online)

increases above 22 cm sediment depth (after ca. 1970).

The CPI values (chl *a*/{chl *a* + pheopigments *a*}; Buchaca and Catalan 2008) calculated through "SDP-CPI" and "HPLC-CPI" approaches match well throughout the sediment profile (Fig. 6d, R^2_{adj} = 0.8, *p*-value = 5.36 * 10^{-09}, n = 25). The CPI values vary within a small range from 0.28 to 0.48 with a positive trend ($p < 0.01$) toward the top of the core. The CPI values do not show a 'tailing' (anomaly) in the topmost centimeters of the sediment with smaller CPI values (less pigment degradation, 'fresher' sediment), suggesting that there is no discernable early diagenetic pigment degradation in the topmost sediment. The CPI values are weakly correlated with the total aquatic production as indicated by chls *a* (r_{adj} = 0.35, *p*-value = 0.045, n = 25).

The ratios of chl *a* to three of the four pheopigments (pyropheophorbide a, pheophorbide *a*, pyrophytin *a*) are > 1.0 throughout the entire core (ESM13), whereas the ratios of chl *a* to pheophytin-*a* are mostly < 1.0 except for the topmost sediment and two samples at the bottom of our sediment core. The correlation between the ratios chl *a*/pyropheophytin *a* and the CPI (r_{adj} = 0.81, *p*-value = 10^{-16}, n = 25), chl *a*/pheophytin *a* and CPI (r_{adj} = 0.73, *p*-value = 10^{-15}, n = 25), chl *a*/pyropheophorbide *a* and CPI (r_{adj} = 0.65, *p*-value = 10^{-15}, n = 25), and chl *a*/pheophorbide *a* and CPI (r_{adj} = 0.35, *p*-value = 10^{-13}, n = 25) are all statistically significant.

Discussion

The goal of this study was to develop a low-cost and rapid method to provide more detailed information about chloropigments (parent and diagenetic compounds) and their use as proxies for aquatic paleoproduction, green algae biomass (Bianchi and Canuel 2011) and chlorophylls preservation (Buchaca and Catalan 2008).

Compared with HPLC analysis, our approach provides less specific pigment information, but it has the advantage to quantify chl *a,* pheopigmnets *a* and, potentially chl *b* in sediment extracts at lower costs and less time (about 20 min measurement and analysis time). The laboratory infrastructure and maintenance is cheaper and staff training is easier. Although substantial development work is still required, the approach could potentially be applied on bulk VIS-VNIR spectra (Butz et al. 2015; Michelutti and Smol 2016) that are obtained directly from sediments without prior pigment extraction. This needs to be explored.

The method validation on standards showed that the INLLS method (Step 1), followed by the application of mono-/dichroic equations (Step 2) allows us to infer chl *a*, chl *b* (parent compounds) and derivatives (pheopigments-a) from bulk spectrophotometer absorption spectra with typical RMSE of 7–11%. In general, chls *b* detection and quantification through INLLS is difficult in the presence of high chls *a* concentration since the molar extinction coefficients of chls *b* are smaller than those of chls *a* in the UV–VIS red range (Jeffrey et al. 1997). From our measurements of the standards it appears that our method is able to accurately quantify chl *b* when the concentration ratio of chl *a*/chl *b* is between 3.41 and 0.16. Higher or lower concentration ratios of chl *a*/chl *b* have not been tested yet and need to be further explored. In our case study of Ponte Tresa, the concentrations of chls *b* are very low (< 10 µg g^{-1}) and the ratio chls *a*/chls *b* is high (> 10; Schneider et al. 2018) which is likely the reason why our approach was not successful to quantify chls *b*. According to the results from the standard solutions, the quantification of chls *b* should be possible with our approach in sediments if the chls *a*/chls *b* ratio is lower than 3.4.

Following Bianchi and Canuel (2011), we diagnose aquatic paleoproduction and, ultimately, eutrophication through the quantification of chls *a*. In our case study of Ponte Tresa (1913–2017, Fig. 6a, c), the eutrophication history as reconstructed by the SDP method compares very well with both the data measured by HPLC and the eutrophication history of Lake Lugano and the Ponte Tresa basin as reported in the literature (Züllig 1982; Barbieri and Mosello 1992; Polli and Simona 1992; Lotter 2001; Lepori and Roberts 2015; Schneider et al. 2018). Oligotrophic/mesotrophic conditions prevailed at the beginning of the twentieth century, eutrophication started in the 1940–1950s, and highly eutrophic conditions persisted from 1964 to the present.

Although it is well established that chlorophyll degradation occurs in the water column and in sediments (Daley and Brown 1973; Carpenter et al. 1986; Hurley and Armstrong 1991), most of the literature focuses on the chlorophyll degradation in the water column (Daley and Brown 1973; Leavitt and Brown 1988; Leavitt 1993). Post-burial pigment degradation, particularly early diagenetic effects in the topmost sediments are still poorly understood. For sedimentary organic matter, Gälman et al. (2008) reported post-burial losses of up to 20% for C and 30% for N within 5 years after deposition. Interpreting the CPI as a proxy for pigment degradation in the water column relies on the assumption that post-sedimentary pigment degradation and early diagenesis is limited, which is likely under anoxic conditions and the absence of light and bioturbation (Bianchi and Canuel 2011). In the sediment of the Ponte Tresa basin, the CPI values of the sediment of the past 100 years (Fig. 6d) do not show an exponential decline towards the sediment surface, as one would expect from early diagenetic degradation of chlorophyll in the top sediments. Similar results were also found in other eutrophic lakes (Deshpande et al. 2014; Makri et al. 2019). The constant CPI values, particularly in the topmost 12 cm (Fig. 6d) suggest that, in the deep Ponte Tresa sub-basin with mostly hypoxic conditions in the hypolimnion, limited light transparency (Secchi depth mostly between 2 and 8 m; at Figino station) and anoxic varved sediment (no bioturbation), early diagenetic transformation of chloropigments is limited, and chloropigments species are well preserved. This is different from well-oxygenated oligotrophic Alpine lakes where trends of chloropigment ratios in the topmost sediments were observed (Guilizzoni et al. 1992).

Conclusions

The purpose of our study was to develop and evaluate the spectral deconvoluted peak SDP approach in order to obtain more information about chloropigments from UV–VIS bulk spectrophotometer absorption spectra of sediment extracts. We applied the approach

on sediment from a lake with a relatively well-known productivity history.

On standard solutions, our mathematical approach is able to quantify chlorophyll *a* and chlorophyll *b* and pheopigments *a* from bulk UV–VIS absorption spectra. The method validation on sediment extracts revealed a RMSE between 3 and 6%. Our approach serves to obtain, in a cost-efficient and time-efficient way, more specific information about sedimentary pigments, which is relevant to infer paleoproduction, Chlorophyll Preservation Index and early diagenetic effects in surface sediments and, potentially, green algae biomass.

In our case study from the Ponte Tresa basin covering the past 100 years, the eutrophication history inferred from our method compares favorably with the eutrophication history as inferred from HPLC measurements and reported in the literature. The CPI values in the topmost sediment suggest that early diagenetic effects are limited and pigments are relatively well preserved once they are buried in anoxic sediments under low light conditions.

Our methodological approach is regarded as a first step towards inexpensive and rapid assessments of sedimentary chlorophylls and their related pheopigments from bulk UV–VIS spectra. In the future, this spectral deconvolution method could, potentially, be applied on bulk UV–VIS spectra measured directly on sediment subsamples or maybe even on entire half-cores.

Acknowledgements This work was supported by the Swiss National Science Foundation (Grant 200021_172586). The authors thank Dr. Andrea Lami for his support with the HPLC method and Dr. Daniela Fischer for laboratory assistance. We thank the two anonymous reviewers and the Associate Editor for thoughtful comments and suggestions.

Author contributions AS and MG designed the research. AS carried out the analytical and methodological work, and AS and MG wrote the paper.

Data accessibility The data are stored at www.pangaea.de.

References

Barbieri A, Mosello R (1992) Chemistry and trophic evolution of Lake Lugano in relation to nutrient budget. Aquat Sci 54:219–237. https://doi.org/10.1007/BF00878138

Belle S, Musazzi S, Lami A (2018) Glacier dynamics influenced carbon flows through lake food webs: evidence from a chironomid δ^{13}C-based reconstruction in the Nepalese Himalayas. Hydrobiologia 809:285–295. https://doi.org/10.1007/s10750-017-3477-8

Bianchi TS, Canuel EA (2011) Chemical biomarkers in aquatic ecosystems. Princeton University Press, Princeton. https://doi.org/10.1515/9781400839100

Brown SB, Houghton JD, Hendry GAF (1991) Chlorophyll breakdown. In: Scheer H (ed) Chlorophylls. CRC Press, Boca Raton, pp 465–489

Buchaca T, Catalan J (2008) On the contribution of phytoplankton and benthic biofilms to the sediment record of marker pigments in high mountain lakes. J Paleolimnol 40:369–383. https://doi.org/10.1007/s10933-007-9167-1

Butz C, Grosjean M, Fischer D, Wunderle S, Tylmann W, Rein B (2015) Hyperspectral imaging spectroscopy: a promising method for the biogeochemical analysis of lake sediments. J Appl Remote Sens 9:096031. https://doi.org/10.1117/1.JRS.9.096031

Carpenter SR, Elser MM, Elser JJ (1986) Chlorophyll production, degradation, and sedimentation: implications for paleolimnology. Limnol Oceanogr 31:112–124. https://doi.org/10.4319/lo.1986.31.1.0112

Daley RJ, Brown SR (1973) Experimental characterization of lacustrine chlorophyll diagenesis. I. Physiological and environmental effects. Arch Hydrobiol 72:277–304

Deshpande BN, Tremblay R, Pienitz R, Vincent WF (2014) Sedimentary pigments as indicators of cyanobacterial dynamics in a hypereutrophic lake. J Paleolimnol 52:171–184. https://doi.org/10.1007/s10933-014-9785-3

Dreßler M, Hübener T, Görs S, Werner P, Selig U (2007) Multiproxy reconstruction of trophic state, hypolimnetic anoxia and phototrophic sulphur bacteria abundance in a dimictic lake in Northern Germany over the past 80 years. J Paleolimnol 37:205–219. https://doi.org/10.1007/s10933-006-9013-x

Gälman V, Rydberg J, de-Luna SS, Bindler R, Renberg I (2008) Carbon and nitrogen loss rates during aging of lake sediment: changes over 27 years studied in varved lake sediment. Limnol Oceanogr 53:1076–1082. https://doi.org/10.4319/lo.2008.53.3.1076

Guilizzoni P, Lami A, Marchetto A (1992) Plant pigment ratios from lakes sediments as indicators of recent acidification in alpine lakes. Limnol Oceanogr 37:1565–1569. https://doi.org/10.4319/lo.1992.37.7.1565

Hurley JP, Armstrong DE (1991) Pigment preservation in lake sediments: a comparison of sedimentary environments in Trout Lake, Wisconsin. Can J Fish Aquat Sci 48:472–486. https://doi.org/10.1139/f91-061

Jeffrey ST, Humphrey GF (1975) New spectrophotometric equations for determining chlorophylls a, b, c1 and c2 in higher plants, algae and natural phytoplankton. Biochem Physiol Pflanz 167:191–194. https://doi.org/10.1016/S0015-3796(17)30778-3

Jeffrey SW, Mantoura RFC, Wright SW (1997) Phytoplankton pigments in oceanography. UNESCO, Paris. https://doi.org/10.1017/S0025315400036389

Küpper H, Seibert S, Parameswaran A (2007) Fast, sensitive, and inexpensive alternative to analytical pigment HPLC: quantification of chlorophylls and carotenoids in crude extracts by fitting with Gauss peak spectra. Anal Chem 79:7611–7627. https://doi.org/10.1021/ac070236m

Lami A, Musazzi S, Marchetto A, Buchaca T, Kernan M, Jeppesen E, Guilizzoni P (2009) Sedimentary pigments in 308 alpine lakes and their relation to environmental gradients. Adv Limnol 62:247–268

Leavitt PR (1993) A review of factors that regulate carotenoid and chlorophyll deposition and fossil pigment abundance. J Paleolimnol 9:109–127. https://doi.org/10.1007/BF00677513

Leavitt PR, Brown SR (1988) Effects of grazing by Daphnia on algal carotenoids: implications for paleolimnology. J Paleolimnol 1:201–213. https://doi.org/10.1007/BF00177766

Lepori F, Roberts JJ (2015) Past and future warming of a deep European lake (Lake Lugano): what are the climatic drivers? J Great Lakes Res 41:973–981. https://doi.org/10.1016/j.jglr.2015.08.004

Lichtenthaler HK (1987) Chlorophylls and carotenoids: pigments of photosynthetic biomembranes. Methods Enzymol 148:350–382. https://doi.org/10.1016/0076-6879(87)48036-1

Lichtenthaler HK, Buschmann C (2001) Chlorophylls and carotenoids: measurement and characterization by UV–VIS spectroscopy. Curr Protoc Food Anal Chem 1:F4.3.1–F4.3.8. https://doi.org/10.1002/0471142913.faf0403s01

Lotter AF (2001) The effect of eutrophication on diatom diversity: examples from six Swiss lakes. In: Jahn R, Kociolek JP, Witkowski A, Compère P (eds) Studies on diatoms. Ganter, Ruggell, pp 417–432

Makri S, Lami A, Lods-Crozet B, Loizeau JL (2019) Reconstruction of trophic state shifts over the past 90 years in a eutrophicated lake in western Switzerland, inferred from the sedimentary record of photosynthetic pigments. J Paleolimnol 61:129–145. https://doi.org/10.1007/s10933-018-0049-5

McGowan S (2013) Pigment studies. In: Elias S, Mock CJ (eds) Encyclopedia of quaternary sciences. Elsevier, Amsterdam, pp 326–338. https://doi.org/10.1016/B978-0-444-53643-3.00235-1

Michelutti N, Smol JP (2016) Visible spectroscopy reliably tracks trends in paleo-production. J Paleolimnol 56:253–265. https://doi.org/10.1007/s10933-016-9921-3

Mikomägi A, Koff T, Martma T, Marzecová A (2016) Biological and geochemical records of human-induced eutrophication in a small hard-water lake. Boreal Environ Res 21:513–527

Naqvi KR, Hassan TH, Naqvi YA (2004) Expeditious implementation of two new methods for analysing the pigment composition of photosynthetic specimens. Spectrochim Acta Part A Mol Biomol Spectrosc 60:2783–2791. https://doi.org/10.1016/j.saa.2004.01.017

Niessen F (1987) Sedimentologische, geophysikalische und geochemische Untersuchungen zur Entstehung und Ablagerungsgeschichte des Luganersees (Schweiz). Doctoral dissertation, ETH Zurich

Nugent JH (1996) Oxygenic photosynthesis: electron transfer in photosystem I and photosystem II. Eur J Biochem 237(3):519–531. https://doi.org/10.1111/j.1432-1033.1996.00519.x

O'Haver T (2016) A pragmatic introduction to signal processing. Lulu Enterprises Incorporated, Morrisville

O'Haver T (2018) Toolkit of functions, scripts and spreadsheet templates. https://terpconnect.umd.edu/~toh/spectrum/peakfit.m. Accessed 30 Mar 2019

Polli B, Simona M (1992) Qualitative and quantitative aspects of the evolution of the planktonic populations in Lake Lugano. Aquat Sci 54:303–320. https://doi.org/10.1007/BF00878143

Ramanathan A, Datta DK, Ghosh P, Kaushal S, Murtugudde R (2012) Tracing nitrogen and carbon biogeochemical processes in the inter-tidal mangrove ecosystem (Sundarban) of India and Bangladesh: implications of the global environmental change. Asia-Pacific Network for Global Change Research. http://www.apn-gcr.org/resources/index.php/items/show/1598

Reuss N, Conley DJ (2005) Effects of sediment storage conditions on pigment analyses. Limnol Oceanogr 3:477–487. https://doi.org/10.4319/lom.2005.3.477

Ritchie RJ (2008) Universal chlorophyll equations for estimating chlorophylls a, b, c, and d and total chlorophylls in natural assemblages of photosynthetic organisms using acetone, methanol, or ethanol solvents. Photosynthetica 46:115–126. https://doi.org/10.1007/s11099-008-0019-7

Routh J, Choudhary P, Meyers PA, Kumar B (2009) A sediment record of recent nutrient loading and trophic state change in Lake Norrviken, Sweden. J Paleolimnol 42:325–341. https://doi.org/10.1007/s10933-008-9279-2

Rutherford AW (1989) Photosystem II, the water-splitting enzyme. Trends Biochem Sci 14:227–232. https://doi.org/10.1016/0968-0004(89)90032-7

Schneider T, Rimer D, Butz C, Grosjean M (2018) A high-resolution pigment and productivity record from the varved Ponte Tresa basin (Lake Lugano, Switzerland) since 1919: insight from an approach that combines hyperspectral imaging and high-performance liquid chromatography. J Paleolimnol 60:381–398. https://doi.org/10.1007/s10933-018-0028-x

Schubert CJ, Niggemann J, Klockgether G, Ferdelman TG (2005) Chlorin index: a new parameter for organic matter freshness in sediments. Geochem Geophys Geosyst. https://doi.org/10.1029/2004GC000837

Simona M (2003) Winter and spring mixing depths affect the trophic status and composition of phytoplankton in the northern meromictic basin of Lake Lugano. J Limnol 62:190–206. https://doi.org/10.4081/jlimnol.2003.190

Thrane JE, Kyle M, Striebel M, Haande S, Grung M, Rohrlack T, Andersen T (2015) Spectrophotometric analysis of pigments: a critical assessment of a high-throughput method for analysis of algal pigment mixtures by spectral deconvolution. PLoS ONE 10(9):e0137645. https://doi.org/10.1371/journal.pone.0137645

Tu L, Jarosch K, Schneider T, Grosjean M (2019) Phosphorus fractions in sediments and their relevance for historical lake eutrophication in the Ponte Tresa basin (Lake Lugano, Switzerland) since 1959. Sci Total Environ 685:806–817. https://doi.org/10.1016/j.scitotenv.2019.06.243

Waters MN, Smoak JM, Saunders CJ (2013) Historic primary producer communities linked to water quality and hydrologic changes in the northern Everglades. J Paleolimnol 49:67–81. https://doi.org/10.1007/s10933-011-9569-y

Welschmeyer NA (1994) Fluorometric analysis of chlorophyll a in the presence of chlorophyll b and pheopigments. Limnol

Oceanogr 39:1985–1992. https://doi.org/10.4319/lo.1994.39.8.1985

Wetzel RG (1970) Recent and postglacial production rates of a marl lake. Limnol Oceanogr 15:491–503. https://doi.org/10.4319/lo.1970.15.4.0491

Züllig H (1982) Untersuchungen über die Stratigraphie von Carotinoiden im geschichteten Sediment von 10 Schweizer Seen zur Erkundung früherer Phytoplankton-entfaltungen. Schweiz Z Hydrol 44:1–98. https://doi.org/10.1007/BF02502191